Journal of Advanced Technology Research Vol.9, No.2, pp.1-7, ISSN: 0974-6269

기능화된 그래핀 및 페닐에틴일 이미드 올리고머 나노복합재의 균열 분석

Fracture in Functionalized Graphene and Phenylethynyl Terminated Imide Oligmer Nanocomposite

Adam McLaughlin[1], 김 병 기(Byungki Kim) [2]*

[1]Department of Mechanical Engineering, University of Massachusetts
One University Ave. Lowell, MA 01854, USA
[2]School of Mechatronics Engineering
Korea University of Technology and Education
*byungki.kim@koreatech.ac.kr

요 약

본 연구에서는 실온에서 기능화된 그래핀 시트(FGS)-페닐에티닐 이미드 올리고머(PETI-5) 복합재의 기계적 특성을 보고한다. 기능화된 그래핀은 PETI-5 복합재의 기계적 특성을 향상시키기 위한 나노필러로 사용된다. 0.08%의 나노필러 질량 분율은 그래핀이 없는 PETI-5 복합재에 비해 파괴 인성이 ~28% 증가한 것으로 나타난다.

키워드 : 페닐에틴일 이미드 올리고머(PETI-5), 파괴 인성, 나노복합체, 기능화된 그래핀 시트

Abstract

In this study, we report the mechanical properties of functionalized graphene sheets (FGSs)-phenylethynyl terminated imide oligomer (PETI-5) composites at room temperature. The functionalized graphene is used as a nanofiller to enhance the mechanical properties of PETI-5 composites. A nanofiller mass fraction of 0.08% shows ~28% increase in fracture toughness compared to PETI-5 composite without graphene.

Keywords : Phenylethynyl terminated imide oligmer (PETI-5), Fracture toughness, Nanocomposites, Functionalized Graphene Sheets

1. INTRODUCTION

The novel mechanical and electrical properties of graphene have been drawing great attention [1-5] . Graphene is an ideal nanofiller for nanocomposites due to its high specific area, high Young's Modulus, and high ultimate strength [6,7] . An increase in storage modulus and glass transition temperature due to the addition of graphene in epoxy was reported by Ramanathan et al. [8] . Yang et al. report that graphene enhances mechanical properties, both impact strength and flexural strength of thermoplastic composite, poly(arylene ethernitrile)-carbon fiber composites at room temperature [9] . A concentration of 5% mass graphene increased the impact strength by 29.4% and the flexural strength by 46.9% compared to a composite without graphene.

PETI-5 was developed by NASA for high-speed transport applications [10-11] . The PETI 5 was developed such that it would not derogate below 600 °C with a high glass transition temperature near 250 °C [10,12] . Because of its superior properties, PETI-5 is being considered as the matrix in a composite cryogenic space shuttle fuel tank. It is also desirable to further enhance the mechanical properties of PETI-5 to prevent microcracking due to thermal cycling. This is planned to be done through the addition of graphene.

2. MATERIALS AND METHODS

2.1. MATERIALS

The functionalized graphene sheets (FGSs) used in this paper were produced through exfoliating graphite as described in our previous paper [14] . The rapid heating of fully oxidized graphite or graphite oxide (GO) produces CO2 and vaporization of water trapped between graphite layers. The gas expansion causes the graphite layers to break apart into individual layers of graphite known as graphene with functional groups. Bulk quantities of exfoliated FGSs with C-O-C (epoxide) and C-OH in oxidized rings and the FGSs terminate with C-OH and -COOH group could be produced through this process [15,16] . The oxygen functionalities of the FGSs help dispersing the FGSs in polar solvents [17,18] .

Phenylethynyl terminated imide oligomer suspended in N-Methyl-2-pyrrolidone (NMP) (Imitec, Inc., NY) was reduced to a PETI-5 powder through rapid precipitation. The

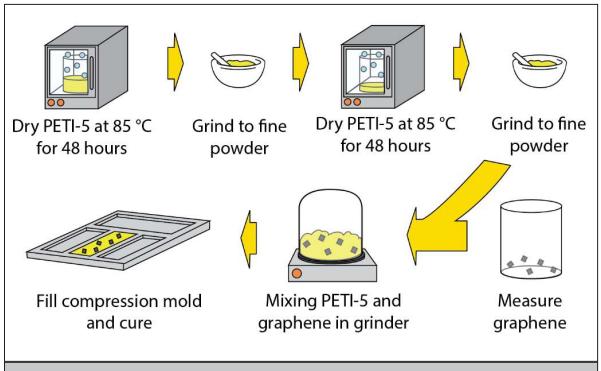

Figure 1. Mixing technique for PETI-5, with graphene nanoparticles.

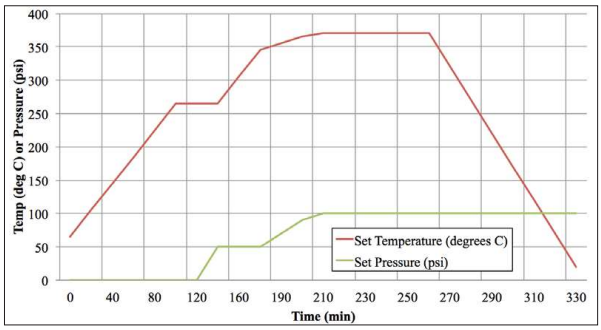

Figure 2. PETI-5 compression mold curing cycle.

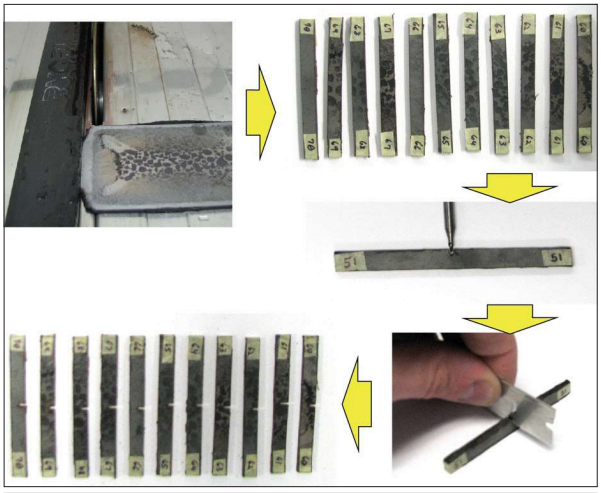

Figure 3. PETI-5 fracture sample production process.

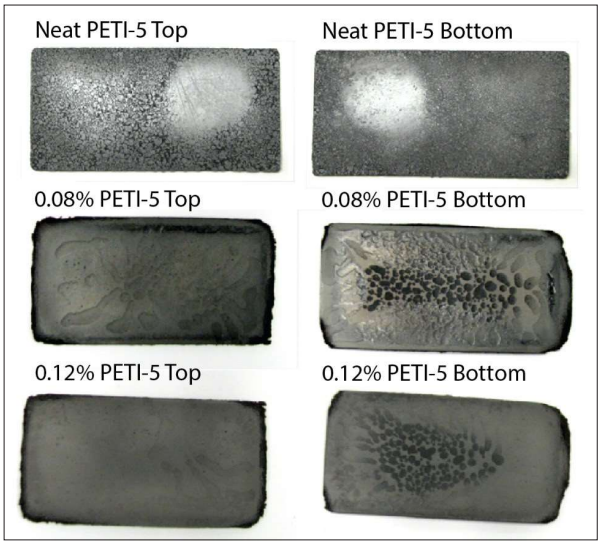

Figure 4. PETI-5 plates produced for fracture testing.

powder was dried in a vacuum oven at 90 °C for 48 hours to remove moisture left behind by the rapid precipitation process. The powder was then ground by hand using a mortar an pestle before being redried in a vacuum oven at 90 °C for 48 hours. The powder was ground again by hand and then used to produce neat PETI-5 plates or graphene nanocomposites. Graphene was measured and added to the PETI-5 where it was mixed using a mechanical grinder (MagicBullet Blender). The final mixture was packed into an aluminum compression mold by hand and then cured in a Dake model 48-197 heated press (DAKE, MI) based on the curing cycle developed by Cho et al. [19] . The mixing and curing process is illustrated in Figure 1 and the Figure 2.

Once cured, the plates were removed from the compression mold and cut using a wet tile saw (WS712, Ryobi Japan) following the ASTM standard D5045-99(2007) for the fracture samples [22]. The pre-crack in the fracture samples were inserted using a Bridgeport Mill (Hardinge Inc., NY) and a 45° mechanical etching bit purchased from Think & Tinker, Ltd (Palmer Lake, CO). Then, a razor was gently pressured into the pre-crack to make a sharp notch. All dimensions were measured with a set of calipers three times and averaged. The sample fabrication process is displayed in Figure 3.

2.2. METHODS

Scanning electron microscopy (SEM, JEOL JSM-1401F FE-SEM) images were captured using neat PETI-5 and 0.08% mass graphene samples. The imaging surfaces were those created by the fracture testing. The SEM was

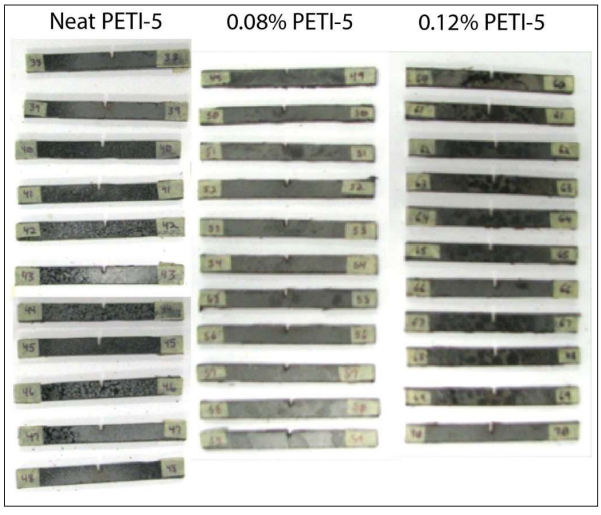

Figure 5. The PETI-5 fracture samples prior to testing.

used with an acceleration voltage of 1 kV, a probe current of 8, and an emission level of 10 μA on low magnification mode with the lower secondary electron detector. The type of fracture, dispersion of graphene, and void content of the PETI-5 samples was observed.

Fracture testing was carried out on an 8511 Instron (Instron, MA) at room temperature. Liquid nitrogen (Airgas, NH) was used to cool the chamber to the cryogenic temperature of -180 °C. Testing was performed according to the D5045-99(2007) ASTM standard. The load head was lowered at a rate of crosshead speed of 0.02794 cm/s (0.011 in/s). Load and displacement was recorded with the Instron Bluehill software.

The fracture toughness, KIC, was determined for each sample according to the D5045-99(2007) ASTM standard.

$$K_{IC} = \frac{P \cdot f\left(\frac{a}{w}\right)}{b \cdot \sqrt{w}} \quad (1)$$

$$f\left(\frac{a}{w}\right) = 6\sqrt{\frac{a}{w}}\left(\frac{1.99 - \frac{a}{w}\left(1-\frac{a}{w}\right)\left(2.15 - 3.93\frac{a}{w} + 2.7\left(\frac{a}{w}\right)^2\right)}{\left(1+2\frac{a}{w}\right)\left(1-\left(\frac{a}{w}\right)^{\frac{3}{2}}\right)}\right) \quad (2)$$

Table 1. Comparison of PETI-5 plate densities.

Sample	ρ (kg/m3)	Percent Difference
Neat PETI-5	1116 ± 10	0%
0.08% Graphene	1226 ± 25	10%
0.12% Graphene	1208 ± 27	8%

Equation (1) was used to determine KIC for each sample. In this equation, P is the maximum load applied in the center of the sample, b is the thickness of the sample, w, is the width of the sample, and a is the initial length of the crack in the sample. The function f(a/w) in Equation (1) was determined using Equation (2).

3. RESULTS

Three PETI-5 plates were produced, each with a concentration of 0%, 0.08%, and 0.12% mass graphene. The plates appeared smooth on the outer surfaces with minor surface defects. Overall, it appeared that the PETI-5 powder had been packed tightly together by the compression mold. The three plates are displayed in Figure 4.

The density of all samples was measured to make ensure comparability of results.

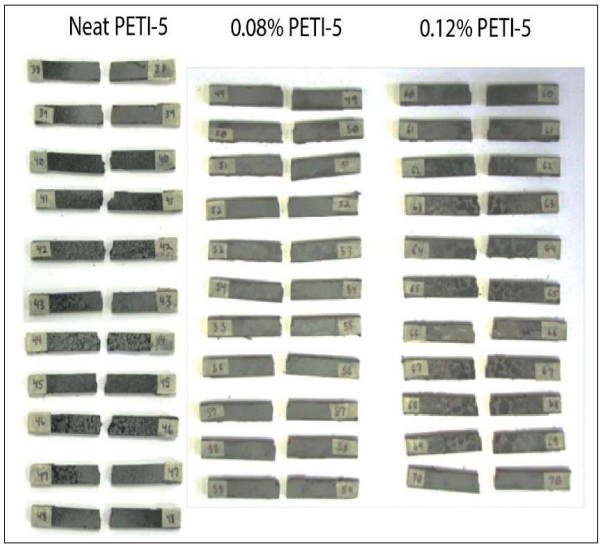

Figure 6. The PETI-5 fracture samples after ultimate failure.

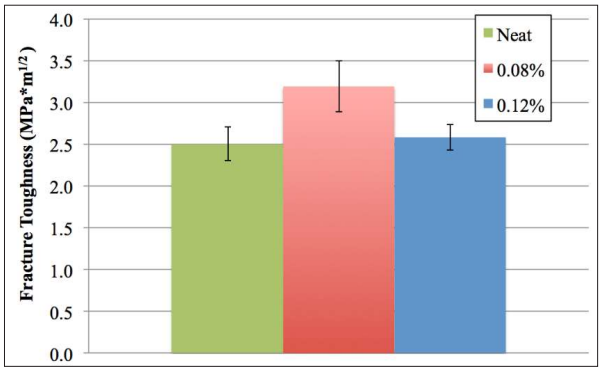

Figure 7. Fracture testing results.

The density was calculated by measuring the dimensions of each sample with calipers and the mass with a scale. The mass was then divided by the volume to determine the density. The density of all samples was within 10% of the neat PETI-5 samples as is displayed in Table 1.

The all cut surfaces appeared smooth and voidless optically. After fracture, some samples exhibited extremely rough fracture surfaces. These samples were assumed to have contained voids and their experimental values were not averaged into the results. The majority of samples exhibited smooth fracture surfaces, which fractured vertically from the base of the pre-crack. The samples before and after testing are arranged in Figure 5 and Figure 6.

Fracture testing shows an increase in fracture toughness at 0.08% mass graphene by 28% over the neat PETI-5 sample. The 0.12% mass graphene sample shows a 3% increase in fracture toughness, however this result is not statistically significant as its error bars overlap with the neat PETI-5 sample. The results are displayed in Figure 7.

SEM imaging revealed two very different fracture surfaces between the neat PETI-5 and 0.08% mass graphene PETI-5 samples. The neat PETI-5 sample exhibited smooth surfaces divided by very pronounced lines of necking. This indicates a ductile failure. The 0.08% mass graphene PETI-5 sample displayed a similar surface except the features were much less pronounced. The lines appear to form around defects on the surface. When these defects are observed closer, they appear to be agglomerates of graphene ranging from 30 to 140 μm in length and 6 to 30 μm in width. The captured SEM images are displayed in Figure 8.

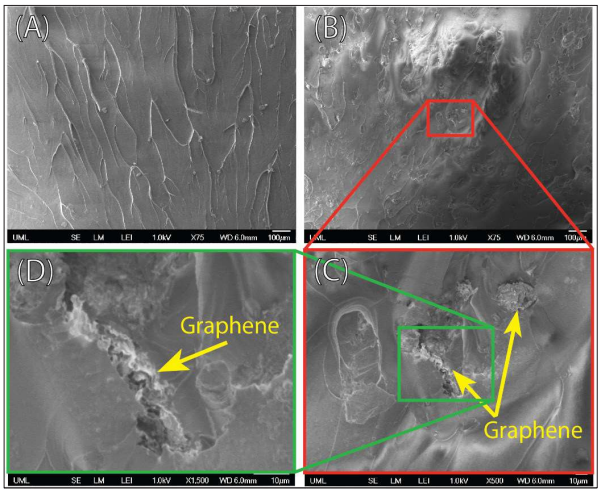

Figure 8. SEM images of the neat PETI-5 fracture surface (A) and the 0.08% mass graphene PETI-5 fracture surface displaying agglomerates of graphene.

4. DISCUSSION

As was seen in our previous report, graphene increases the fracture toughness of a matrix up to a certain concentration of graphene. Above this concentration of graphene, the fracture toughness decreases to or below the fracture toughness of the sample without graphene. Based on our previous paper, the 0.08% mass graphene was identified as the ideal concentration of graphene to produce the maximum fracture toughness in a carbon fiber reinforced polymer composite.

Of the graphene concentrations tested in PETI-5, the 0.08% mass graphene sample had the highest fracture toughness showing a statistically significant increase of 28% over the neat PETI-5 sample. The higher concentration of graphene returns to approximately the same value as the neat PETI-5. It is believed that at the higher concentration of graphene, the nanoparticle acts as a defect due to larger aggregates. For this reason, the fracture toughness decreases.

The SEM images indicate that the graphene

greatly affects the fracture surface of the nanocomposites. The neat PETI-5 fracture sample displays a smooth surface with extremely pronounced lines running through the sample. The 0.08% mass graphene appears rougher, with less pronounced lines encircling graphene agglomerates. The neat PETI-5 appears quasi-brittle, while the 0.08% mass graphene sample appears more ductile. This is consistent with the increase in fracture toughness observed through mechanical testing.

The graphene does appear to form large agglomerates with the current mixing process. This should be studied more and a larger range of graphene concentrations should be tested to identify the ideal level of graphene in a PETI-5 composite.

5. CONCLUSIONS

A concentration of 0.08% mass graphene yielded a 28% increase in fracture toughness at room temperature over neat PETI-5. Higher concentrations of graphene do not improve the fracture toughness of the PETI-5 by a statistically significant amount. The addition of graphene increased the ductility of the PETI-5 as is evident by the fracture surfaces observed through SEM. Large graphene agglomerates were present in the PETI-5 sample. It may be beneficial to improve the mixing process for maximum mechanical properties.

REFERENCES

[1] C. Lee, X. Wei, J. W. Kysar, J. Hone, Science. 2008, 321, 385-388.

[2] D. Li, R. B. Kaner, Science. 2008, 320, 1170-1171.

[3] A. K. Geim, K. S. Novoselov, Nat Mater. 2007, 6, 183-191.

[4] D. C. Elias, R. R. Nair, T. M. G. Mohiuddin, S. V. Morozov, P. Blake, M. P. Halsall, A. C. Ferrari, D. W. Boukhvalov, M. I. Katsnelson, A. K. Geim, K. S. Novoselov, Science. 2009, 323, 610-613.

[5] S. Y. Zhou, G. -. Gweon, A. V. Fedorov, P. N. First, W. A. de Heer, D. -. Lee, F. Guinea, A. H. Castro Neto, A. Lanzara, Nat Mater. 2007, 6, 770-775.

[6] R. J. Young, I. A. Kinloch, L. Gong, K. S. Novoselov, Composites Sci. Technol. 2012, 72, 1459-1476.

[7] D. Cai, J. Jin, K. Yusoh, R. Rafiq, M. Song, Composites Science and Technology. , 702.

[8] RamanathanT., AbdalaA. A., StankovichS., DikinD. A., Herrera-AlonsoM., PinerR. D., AdamsonD. H., SchnieppH. C., ChenX., RuoffR. S., NguyenS. T., AksayI. A., Prud'HommeR. K., BrinsonL. C., Nat Nano. 2008, 3, 327-331.

[9] X. Yang, Z. Wang, M. Xu, R. Zhao, X. Liu, Mater Des. 2013, 44, 74-80.

[10] Y. Tang, Y. Xie, W. Pan, A. Riga, Thermochimica Acta. 2000, 357–358, 239-249.

[11] M. M. Pavlick, W. S. Johnson, B. Jensen, E. Weiser, Composites Part A: Applied Science and Manufacturing. 2009, 40, 359-367.

[12] D. Lee, H. V. Tippur, B. J. Jensen, P. B. Bogert, Engineering Material Technology. 2011, 133.

[13] M. Kim, J. Hong, S. Kang, C. Kim, Composites Part A: Applied Science and Manufacturing; Fifth Asianâ€“Australian

Conference on Composite Materials (ACCM-5) Fifth Asianâ€“Australian Conference on Composite Materials. 2008, 39, 647-654.

[14] J. K. Lee, S. Song, B. Kim, Polymer Composites. 2012, 33, 1263-1273.

[15] H. C. Schniepp, J. Li, M. J. McAllister, H. Sai, M. Herrera-Alonso, D. H. Adamson, R. K. Prud'homme, R. Car, D. A. Saville, I. A. Aksay, J Phys Chem B. 2006, 110, 8535-8539.

[16] M. J. McAllister, J. Li, D. H. Adamson, H. C. Schniepp, A. A. Abdala, J. Liu, M. Herrera-Alonso, D. L. Milius, R. Car, R. K. Prud'homme, I. A. Aksay, Chem. Mater. 2007, 19, 4396-4404.

[17] S. Stankovich, R. D. Piner, S. T. Nguyen, R. S. Ruoff, Carbon. 2006, 44, 3342-3347.

[18] S. Park, J. An, I. Jung, R. D. Piner, S. J. An, X. Li, A. Velamakanni, R. S. Ruoff, Nano Lett. 2009, 9, 1593-1597.

[19] D. Cho, S. Lee, G. Yang, H. Fukushima, L. T. Drzal, Macromolecular Materials and Engineering. 2005, 290, 179-187.